Mehmet Akif Ersoy Üniversitesi Uygulamalı Bilimler Dergisi
Journal of Applied Sciences of Mehmet Akif Ersoy University

The Investigation of the Effects of Different Filters on Mammogram Images

Ayşe Aydın Yurdusev[1*], Canan Oral[2], Mahmut Hekim[3]

[1]Research Asst., Amasya University, Technology Faculty, Department of Electrical and Electronics Engineering

[2]Dr. Öğr. Üyesi, Amasya University, Technology Faculty, Department of Electrical and Electronics Engineering

[3]Assoc.Prof.Dr., Gaziosmanpaşa University, Fac. of Engineering, Dep.of Electrical and Electronics Engineering

Geliş Tarihi/Received: 25.10.2017
Kabul Tarihi/Accepted: 10.12.2017 Araştırma Makalesi/Research Article

ABSTRACT

Mammography is a widespread imaging technique to early detect breast cancer. It can detect micro scale calcium deposits (microcalcification) known as early signs of breast cancer. The detection of microcalcifications on mammograms, computer-aided diagnosis (CAD) systems is commonly used. The first step of CAD system is cleaning noises on mammography images. In order to clean or decrease noise on images, several filters are used. The purpose of this study is denoising mammogram images that include microcalcification with different filters and comparing of filter results. For this, firstly 50 mammogram images are obtained from Digital Database for Screening Mammography (DDSM). Microcalcification located areas which stated in their data file on mammograms are cropped at 512x512 pixels. Each image matrices are filtered by median and moving average filter in spatial domain as well as high pass and low pass filter in frequency domain. The filtered images are compared by mean square error (MSE) and peak signal-noise ratio (PSNR) after frequency domain filters contrast adjustment. As a result the optimal filter will be determined for cleaning mammograms without an effect on single or clustered microcalcification.

Keywords: Mammogram, Microcalcification, Filtering on frequency domain, Filtering on spatial domain, Denoising.

Mamogram İmgeleri Üzerinde Farklı Süzgeçlerin Etkilerinin İncelenmesi

ÖZET

Mamaografi meme kanserinin erken teşhisi için kullanılan yaygın bir görüntüleme tekniğidir ve meme kanserinin başlangıç aşaması olarak kabul edilen küçük kalsiyum birikintilerini

* Sorumlu yazar/Corresponding author
E-mail/e-ileti: ayse.yurdusev@amasya.edu.tr

(mikrokalsifikasyonlar) görüntüleyebilme özelliğine sahiptir. Mikrokalsifikasyonların mamografi üzerindeki tespitleri için bilgisayar destekli tespit (BDT) sistemleri sıklıkla kullanılmaktadır. BDT sistemlerin ilk basamağı mamografi üzerinde oluşan gürültüleri temizlemektir. Gürültü temizleme veya azaltma işlemi için çeşitli süzgeçler kullanılmaktadır. Bu çalışmada mikrokalsifikasyon içeren mamografi görüntülerin çeşitli süzgeçlerle temizlenmesi ve sonuçlarının karşılaştırılması hedeflenmektedir. Bunun için öncelikle Digital Database for Screening Mammography (DDSM) veritabanındaki mamografilerden mikrokalsifikasyon içeren 50 adet mamografi imgesi seçilmiştir. Alınan mamografilerden mikrokalsifikasyon içeren kısımları vertabanında verilen koordnatlar ile 512x512 piksel boyutunda kesilmiştir. Her bir görüntü matrisi uzamsal bölgede ortanca ve ortalama süzgeçten, frekans bölgesinde ise alçak geçiren ve yüksek geçiren süzgeçlerden geçirilerek kontrast ayarlanmış görüntü sonuçları ortalama hata karesi ve doruk işaret-gürültü oranı ile karşılaştırılmıştır. Çalışma sonucunda tek mikrokalsifikasyonlara ve mikrokalsifikasyon gruplarına etki etmeden, mamografilerde gürültü temizlemek için en uygun süzgecinin hangisi olduğu tespit edilecektir.

Anahtar kelimeler: Mamaografi, Mikrokalsifikasyon, Frekans Bölgesinde Süzme, Uzamsal Bölgede Süzme, Süzgeç.

1. INTRODUCTION

Breast cancer is one of the most fatal cancer types, due to its proximity to vital organs such as lymph. According to statistics, approximately 40000 women will die caused by breast cancer or breast cancer-related symptoms in each year (Murthy et al., 2016). Hence, early detection of breast cancer is most predictive factors to inhibit deaths related to breast cancer. Mammography is a most significant method for screening and detection of breast cancer (Memiş, 2002; Avdan, 2013; Akbay, 2015; Redman et al., 2015). It can detect micro scale calcifications, termed as microcalcification, on the breast. Microcalcifications are assumed as very first sign of breast cancer. The existence of microcalcifications is vital to perceive breast cancer in early detection (Memiş, 2002). Hence, interpretation of mammograms has critical importance.

Computer-aided diagnosis (CAD) system can help to improve the proportions of success about cancer detection. Because even experienced radiologists may miss signs of microcalcification due to their dimensions and locations. Incorrectly labeled mammograms may cause undetected severe cancer. On the other hand, unnecessary biopsies and further medical examinations may cause to purchase redundant healthcare sources as well as may place a great burden on patients (Qian et al., 2015). In the literature, there are numerous studies and algorithms of CAD systems (Shen et al., 1994; Kim et al., 1997; Kim and Park, 1999; Soltanian-Zadeh et al., 2004; Fu et al., 2005; Kurt and Nabiyev, 2010; Pak et al., 2015). In order to achieve higher true labelling proportion on mammograms, preprocessing of mammogram images is necessary. Since each mammogram images have the uncertain and unpredictable amount of noise that most of them occur by quantum noise (Romualdo et al., 2009). Quantum noise, especially affects the visibility of microcalcifications on mammograms, as microcalcifications are tiny particles that are sized about 100µm to 500µm (Romualdo et al., 2009).

Kumar et al. conducted a study with 10 mammogram images from MIAS database. They cropped images 128x128 pixels and applied Adaptive Histogram Equalization (AHE), Median filter, Frost filter, Butterworth filter and Wavelet denoising filter. Each image was evaluated by mean square error (MSE), peak-signal to noise ratio (PSNR), Mean Structure Similarity Index (MSSIM), Maximum difference (MD), Normalized Absolute Error (NAE) and Structural Content (SC). According to their study results, most preferable filters are determined as median filter and wavelet denoising filter (Kumar et al., 2016). Vijikala et al. analyzed 5 different filter algorithms, namely Hybrid Median Filter (HMF), Linear Minimum Mean Square Error (LMMSE) Filter, Oriented Rician Noise Reduction Anisotropic Diffusion (ORNRAD) Filter, Higher Order Filter (HOF), Non-Local Means (NLM) Filter on noiseless and Rician noise added mammogram images. Filtered images are compared with MSE, PNSR, Contrast to Noise Ratio (CNR), Quality Index (IQI) and Mean Absolute Error (MAE) values. The results show that ORNRAD filter results have higher ratio to succeed (Vijikala et al.) Nagaiah et al. conducted a study to determine best enhancement method for mammogram analysis. They computed 30 mammogram images from MIAS database. Firstly, they add some noise on mammograms such as salt and pepper, Gaussian, Speckle and Poisson noise. After that noise added images filtered by Inverse T/F filter known as low-pass filter, Median Filter, and Bileteral filter. The results are examined by MSE and PNSR values. According to their study Inverse T/F filter achieved better enhancement than others (Nagaiah et al., 2016).

The aim of this study, evaluation of effects of filters on microcalcifications. The study is performed on 50 mammogram images from DDSM database. Each mammogram images are cropped in the region of interest. Then salt & pepper noise and Gaussian noise are added to original images. Noise-free images and noisy images are filtered by median filter, moving average filter, low-pass filter and high-pass filter. The performance of the filtering processes is evaluated by MSE and PNSR.

2. MATERIAL AND METHOD

DDSM database one of the well-known mammographic images database. It has 2620 cases, each case has four mamogram images; specifically, right mediolateral-oblique (MLO), right Cranial-Caudal (CC), left MLO, left CC views. Each of them labelled with patients' condition such as cancer, benign and normal. Moreover, abnormal tissues are demonstrated with a chain code. Mammogram images have a resolution of 42 microns to 50 microns and 12-16 bit depth depended on their scanner brand and they have different dimensions (Heath et al., 2001).

In this study, 50 cancer cases with microcalcification are chosen from DDSM database. 50 percent of them are selected by MLO view and others taken by CC view. All selected mammograms are obtained by HOWTEK scanner mammograms with 43.5 microns resolution and 12-bit depth. Mammogram images are cropped by based on given chain codes at 512x512 pixels that is the approximately 2x2cm^2 area.

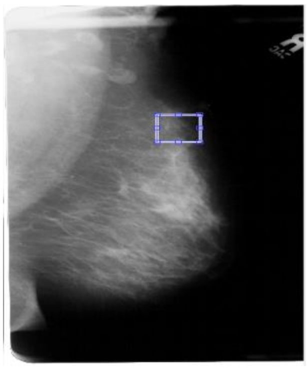

Figure 1. A_1258_1.RIGHT_MLO view mammogram.

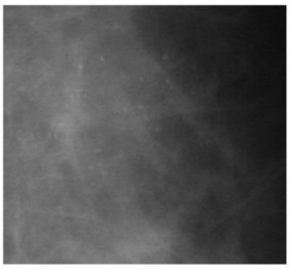

Figure 2. A_1258_1.RIGHT_MLO cropped microcalcification region

Figure 1. demonstrates that an original mammogram view. Size of the image is 6871x3541 pixels. Microcalcifications areas are illustrated with a blue rectangle. Figure 2. shows only microcalcification region, the region of interest (ROI), from mammogram with the dimension of 512x512 pixels. Microcalcification cluster can be seen from it.

Figure 3. indicates proposed block diagram. Firstly, prepared mammogram images are added with salt & pepper and Gaussian noises. Then original and noisy mammogram images are filtered by spatial domain filters and frequency domain filters. Their results are compared with MSE and PNSR values.

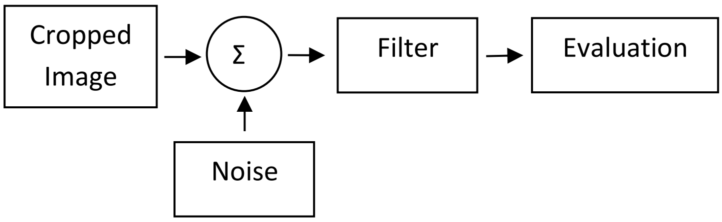

Figure 3. Algorithm of the study

3. TYPE OF IMAGE NOISES

On digital mammograms, noise is one of the most challenging issues. Noise can change pixel intensities and can cause to misinterpretation (Romualdo et al., 2009; Veldkamp and Karssemeijer, 2000; Gonzalez et al., 2014). Because deciding most preferable filter, mammogram images may be degenerated with same types of noises. Then they filtered by filters and the result are compared (Vijikala et al.; Nagaiah et al., 2016).

3.1. Salt and Pepper Noise

On an image, salt and pepper noise changes some pixels with minimum or maximum intensities randomly. Also, it is known as impulse noise. This type of noise can be seen in digital imagining systems converting of scanner data to image is quicker (Gonzalez et al., 2014).

Figure 4. shows the selected mammogram which has additive salt and pepper noise that minimum (0 intensities, black pixels named as peppers) and maximum (1 intensities, white pixels named as salt) pixels are added to the image.

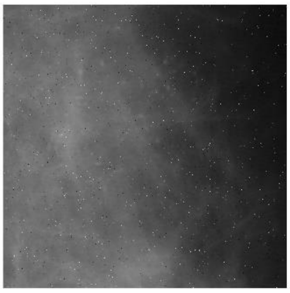

Figure 4. Mammogram with Salt&Pepper Noise

3.2. Gaussian Noise

Gaussian noise is widely used for image processing. The distribution of it is normal (Gonzalez et al., 2014; Starck and Murtagh, 2006). The formula of the probability density function of gauss noise is given by equation 1. Where z is pixel intensity and σ is variance.

$$p(z) = \frac{1}{\sqrt{2\pi\sigma}} e^{-(z-\bar{z})^2 / 2\sigma^2} \quad (1)$$

The image is added Gaussian noise can be seen in Figure 5. Image has gray-level contamination all its around, that creates a fuzzier image.

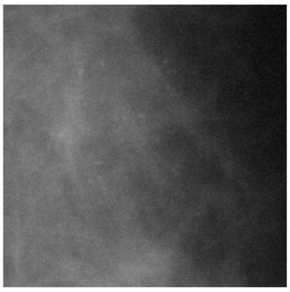

Figure 5. Mammogram with Gaussian Noise

4. TYPE OF IMAGE FILTERS

Image filters are used to make images clearer, sharpener or less noisy. The filter concept is based on suppressing some content to enhance others (Gonzalez et al., 2014). Fundamentally there are 2 types of image filtering. Firstly, spatial domain filtering that is directly applied pixel values. Frequency domain filtering is applied to image in frequency domain and then image is recreated in spatial domain. Figure 6. shows the image filtering concept.

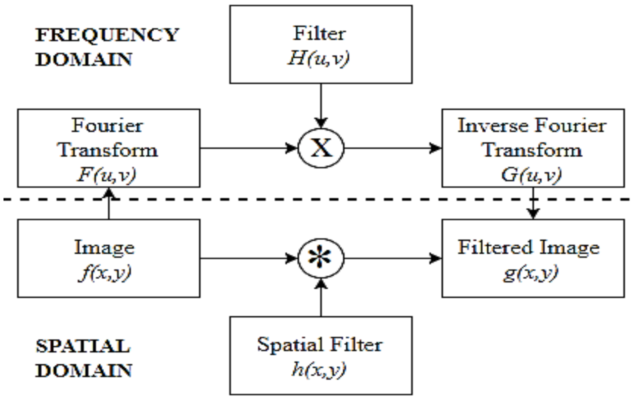

Figure 6. Image filtering concept

4.1. Median Filter

Median filter computes a center pixel and its neighborhoods relationship. It lists a kernel values in order and replaces middle value to center pixel. Hence, the differentiation between pixels is declined. Therefore the image become more smooth and clearer.

Table 1. Example Image matrix

100	150	200
150	**250**	110
200	150	150

As an example, Table 1. indicates an image matrix. When the 3x3 median filter is adapted to the matrix, the middle pixel which has a a value of 250 became 150. Hence, values of the matrix are sorted respectively:

100 110 150 150 <u>150</u> 150 200 200 250

The middle value is 150, it replaces to center pixel.

4.2. Moving Average Filter

Moving window filter (MWF), is a moving average filter (MAF) for 2-dimension, replaces the value of the center pixel of the kernel with an an average value of kernel. Where f(i,j) is image pixel and g(i,j) is center pixel of kernel, for (2m+1)x(2m+1) filter sized the formulation of MAF is (Gonzalez et al., 2014; Glasbey and Horgan, 1995). :

$$g_{ij} = \frac{1}{mm} \sum_{k=-m}^{m} \sum_{l=-m}^{m} f_{i+k,j+l} \tag{2}$$

Table 1. center pixel becomes 162.22

4.3. Low-Pass Filter

Low-pass filter on frequency domain, suppress higher frequency components than cut-off of the signal while passes lower frequency (Gonzalez et al., 2014). Where D_0 is cut-off frequency, D(u,v) is the proximity of (u,v) pixel location to frequency rectangle. H(u,v) is Gaussian low-pass filter (GLPF) (et al., 2014) :

$$H(u,v) = e^{-\frac{D^2(u,v)}{2D_0^2}} \tag{3}$$

Despite there is an ideal low-pass filter, GLPF can be interpreted due to less ringing effect than an ideal low-pass filter.

4.4. High-Pass Filter

On frequency domain, a high-pass filter attenuates lower that cut-off frequency components and passes high frequencies. It is the complement of the low-pass filter. Hence Gaussian high-pass filter (GHPF) can be introduced as (Gonzalez et al., 2014). :

$$H_{HP}(u,v) = 1 - H_{LP}(u,v) \tag{4}$$

Hence GHPF transfer function is;

$$H(u,v) = 1 - e^{-\frac{D^2(u,v)}{2D_0^2}} \tag{5}$$

In general, the noise component of an image is assumed as high frequency. A high pass filter suppresses low frequencies and passes high frequencies. Hence high pass filters may allow for the presence of noise components. However, high pass filter can emphasize details on the image.

5. EXPERIMENTAL RESULTS

Preprocessed mammograms, firstly, are contaminated with salt and pepper noise and Gaussian noise. After that, original mammograms, salt and pepper noisy mammograms, Gaussian noisy mammograms and both salt and pepper and Gaussian noise affected mammogram are filtered by median filter, MAF, GLPF and GHPF. Filtered mammograms and original mammograms are compared with MSE and PNSR.

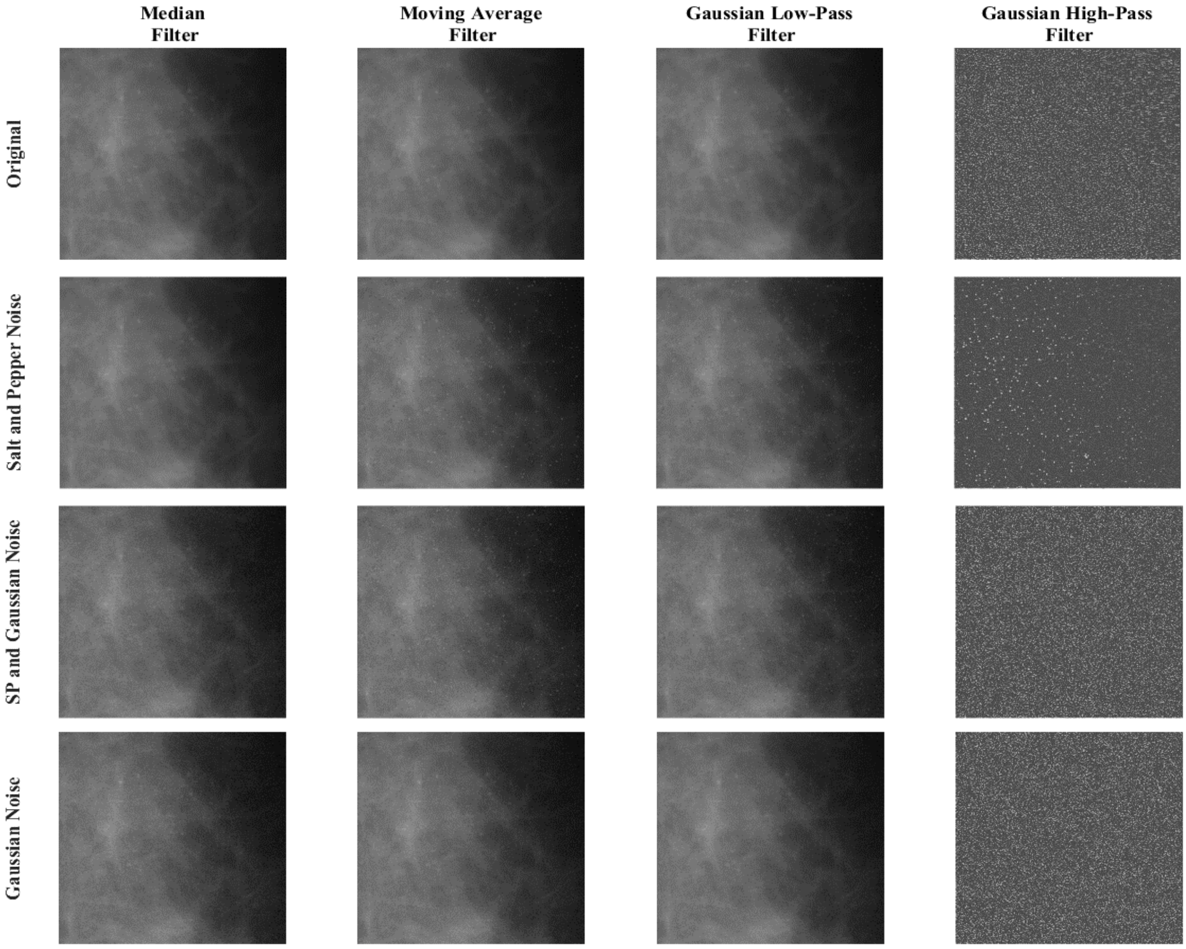

Figure 7. Mammogram ROI with additive noises and applied filters

Original mammograms, noise added mammograms and filtered images can be seen in Figure 7. Top row indicates the applied filter and left line demonstrates additive noises. The noisy images and less noisy images can be seen with naked eyes. Median filter, MAF, and GLPF can enhance the image, however, GHPF emphasizes the expression of noise. Despite it's the impracticality of the reduction of noise level, GHPF is studied in this paper. Because it can be contributed to the study to understand of filters.

The performance of the filters is based on MSE and PNSR values. Basically, MSE computes the similarity between two images. In this study, noisy images are denoised by different filters, the filtered image should be similar to the the original image.

In literature, MSE is often used for image evaluation. The mathematical formulation of MSE is (Singh et al., 2008). :

$$MSE = \frac{1}{MN}\sum_{i=1}^{M}\sum_{j=1}^{N}(I_{(i,j)} - \bar{I}_{(i,j)})^2 \tag{6}$$

Where for MxN pixels sized image $I_{(i,j)}$ is the intensity of original image pixel at ij coordinate, $I_{(i,j)}$ is filtered image value.

PNSR, is peak noise-to-signal ratio, it measures peak error of between two images (Singh et al., 2008).

$$PSNR = 20 * \log\left(\frac{I_{peak}}{\sqrt{MSE}}\right) \tag{7}$$

Where I_{peak} is the possible maximum intensity of the image. That depends on the data type of images, for instance, 8 bits integer's maximum value is 255.

For two identical images, MSE value will be zero and PSNR value will be infinite. Hence, in this study, smaller MSE values and higher PSNR values are the best.

The distribution of PNSR values can be seen in Figure 8. PNSR and MSE values are calculated for 16 iterations, 4 types of noise and 4 types of filter, for each mammogram. For instance, noise free mammograms filtered by median filter and their PSNR values are between 52dB to 46dB with an average value of 49dB.

According to Figure 8., the worst values are related to GHPF, as expected. Because, Figure 7, also, shows that between original mammogram and GHFP mammograms have high dissimilarity. Noisy mammograms, without filtering, have lower PNSR values about 25-30dB. It is meaning that all filters are effective except GHPF.

On salt & pepper noise added mammograms, median filter gives the more attractive results, which are the same with original images values. For the Gaussian noised image, most improvement is occurred by GLPF. When both salt & pepper noise and Gaussian noise are added to mammograms, Median filter and GLPF show similar PNSR values about 36dB. However, using both median filter and GLPF for salt & pepper and Gaussian noise added mammogram presents a slight enhancement of PNSR values.

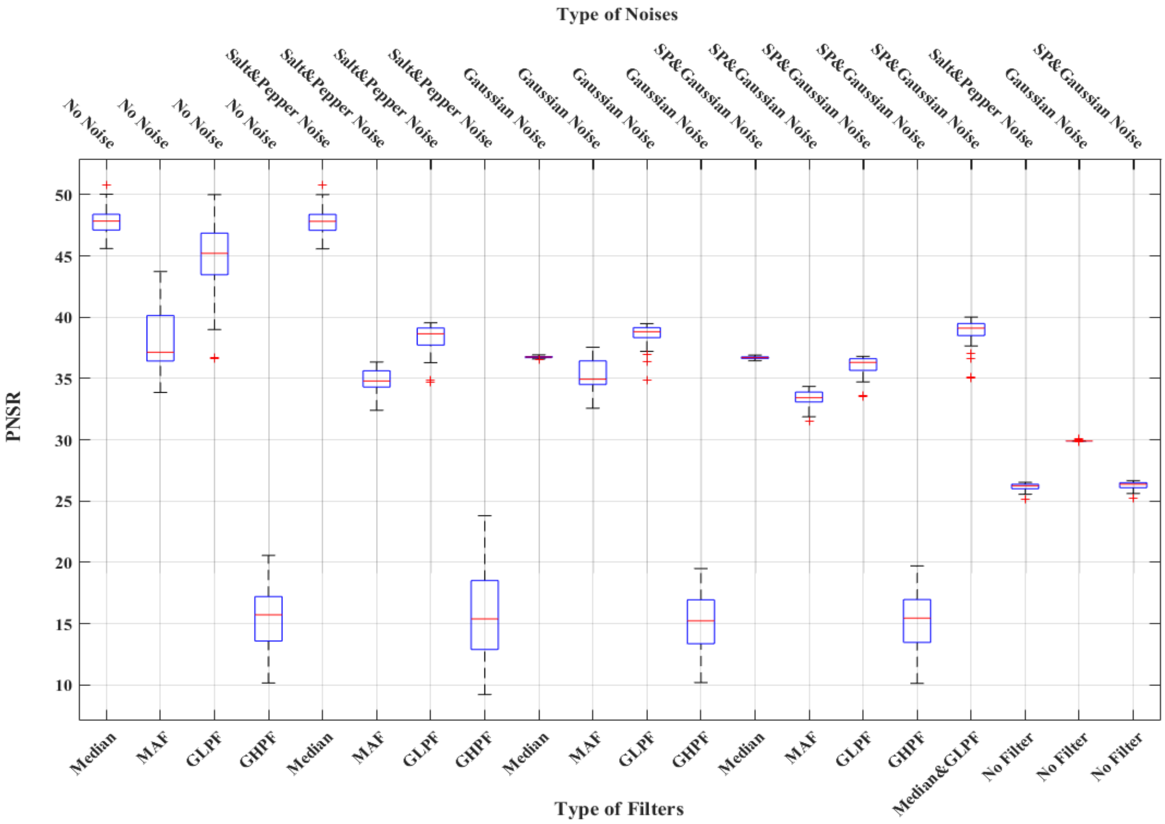

Figure 8. The distribution of PNSR

The MSE evaluation of filters on mammograms can be seen in Figure 9. for MSE values, mammograms that are filtered by GHPFs and original mammograms do not include the chart, due to their significantly higher MSE value.

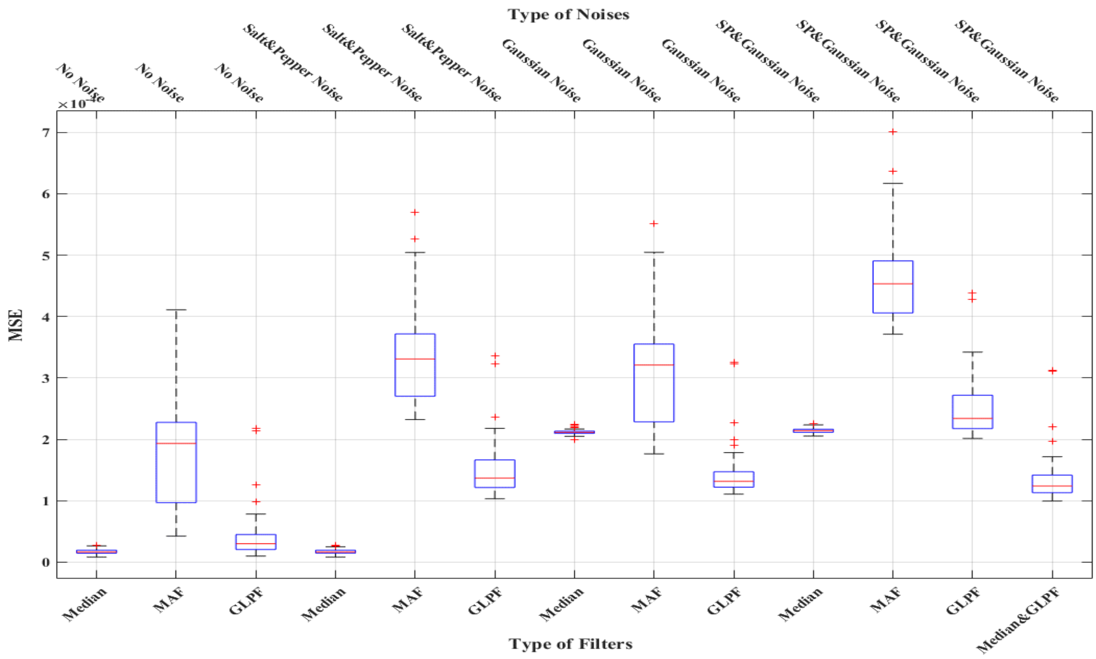

Figure 9. The distribution of MSE

It can be seen in Figure 9. the best results obtained by median filter and GLPF. For no noise added mammograms, median filter and GLPF decrease to the value of $1x10^{-4}$.

For all noise types, MAF has slightly higher MSE values than Median filter and GLPF. However, it shows better results than unfiltered ones.

6. RESULTS AND DISCUSSION

The most important aim of this study to investigate filtering effects on mammograms keep microcalcification. Therefore, denoised images are evaluated by MSE and PNSR. The evaluation values show that mammograms still have close similarity after denoising algorithm.

In this study, different filters effects are investigated for mammograms. According to implementation results, using both median filter and GLPF have more successful similarity rates than others. As a result, using these two filters together can reduce the noise level without changing the characteristic of microcalsifications clusters on digital mammograms.

Acknowledgment

This study is supported by Amasya University Scientific Research Projects (BAP) Unit (Project Number FMB-BAP 16-0181).

References

Avdan, A. A. (2013). Duktal Karsinoma İn Situ'da BI-RADS Tanımlayıcıları İle Moleküler Prognostik Faktörler Arasındaki İlişki, GAZİ ÜNİVERSİTESİ TIP.

Memiş, A. (2002). Meme Radyolojisi.

Redman, A., Lowes, S. and Leaver, A. (2015). Imaging techniques in breast cancer, Surg. (United Kingdom), 34(1), 8–18.

Kurt, B. and Nabiyev, V. V. (2010). Dijital Mamografi Görüntülerinin Kontrast Sınırlı Adaptif Histogram Eşitleme ile İyileştirilmesi, *VII. Ulusal Tıp Bilişimi Kongresi*, 67–78.

Akbay, C. (2015). Applicatıon Of Image Enhancement Algorithms To Improve The Visibility And Classification Of Microcalcifications In Mammograms, MIDDLE EAST TECHNICAL UNIVERSITY.

Glasbey, C. A. and Horgan, G. W. (1995). *Image Analysis for the Biological Sciences*, 1. edition. University of Michigan: Wiley.

Pak, F., Kanan, H. R. and Alikhassi A. (2015). Breast cancer detection and classification in digital mammography based on Non-Subsampled Contourlet Transform (NSCT) and Super Resolution, *Comput. Methods Programs Biomed.*, 122(2), 89–107.

Soltanian-Zadeh, H., Rafiee-Rad, F. and Pourabdollah-Nejad, D. S. (2004). Comparison of multiwavelet, wavelet, Haralick, and shape features for microcalcification classification in mammograms, *Pattern Recognit.*, 37(10), 1973–1986.

Fu, J. C., Lee, S. K., Wong, S. T. C., Yeh, J. Y., Wang, A. H. and Wu, H. K. (2005). Image segmentation feature selection and pattern classification for mammographic microcalcifications, *Comput. Med. Imaging Graph.*, 29(6), 419–429.

Kim, J. K. and Park, H. W. (1999). Statistical textural features for detection of microcalcifications in digitized mammograms, *IEEE Trans. Med. Imaging*, 18(3), 231–238.

Kim, J. K., Park, J. M., Song, K. S. and Park, H. W. (1997). Adaptive mammographic image enhancement using first derivative and local statistics, *Med. Imaging, IEEE Trans.*, 16(5), 495–502.

Starck J. and Murtagh, F. (2006). Handbook of Astronomical Data Analysis, *Analysis*, 338.

Nagaiah, K., Manjunathachari, K. and Rajinikanth, T. V. (2016). Advanced image enhancement method for mammogram analysis, *2016 Int. Conf. Recent Trends Inf. Technol.*, 1–5.

Romualdo, L. C. D. S., Vieira, M. A. D. C. and Schiabel, H. (2009). Mammography images restoration by quantum noise reduction and inverse MTF filtering, *Proc. SIBGRAPI 2009 - 22nd Brazilian Symp. Comput. Graph. Image Process.*, 1, 180–185.

Shen, L., Rangayyan, R. M. and Desautels, J. E. L. (1994). Application of Shape-Analysis to Mammographic Calcifications," *IEEE Trans. Med. Imaging*, 13(2), 263–274.

Heath, M., Bowyer, K., Kopans, D., Moore, R. and Kegelmeyer, W. P. (2001). The Digital Database for Screening Mammography, in *Proceedings of the Fifth International Workshop on Digital Mammography*, 212–218.

Kumar, M., Thakkar, V. M., Bhadauria, H. S., Kumar, I., Pant, G. B. and College, E. (2016). Mammogram's Denoising in Spatial and Frequency Domain, October, 654–659.

Gonzalez, R. C., Woods, R. E., Telatar, Z., Tora, H., Arı, H. and Kalaycıoğlu, A. (2014). *Sayısal Görüntü İşleme*. Ankara: Palme Yayıncılık.

Murthy, R. K., Valero, V. and Buchholz, T. A. (2016). Breast Cancer, *Clin. Radiat. Oncol.*, 1284–1302.

Singh, V., Rajpal, N. and Murthy, K. S. (2008). A Neuro Fuzzy Model for Image Compression in Wavelet Domain," in *Image and Signal Processing: 3rd International Conference, ICISP 2008. Cherbourg-Octeville, France, July 1 - 3, 2008. Proceedings*, A. Elmoataz, O. Lezoray, F. Nouboud, and D. Mammass, Eds. Berlin, Heidelberg: Springer Berlin Heidelberg, 46–58.

Vijikala, V., Jyothi, V. and College, E. IDENTIFICATION OF MOST PREFERENTIAL DENOISING METHOD FOR MAMMOGRAM.

Veldkamp, W. J. H. and Karssemeijer, N. (2000). Normalization of local contrast in mammograms, *IEEE Trans. Med. Imaging*, 19(7), 731–738.

Qian, W., Sun, W. and Zheng, B. (2015). Improving the efficacy of mammography screening: the potential and challenge of developing new computer-aided detection approaches., *Expert Rev. Med. Devices*, 12(5), 497–499.